JEE Journal of Ecological Engineering

Journal of Ecological Engineering 2023, 24(7), 274–284
https://doi.org/10.12911/22998993/165781
ISSN 2299–8993, License CC-BY 4.0

Received: 2023.04.21
Accepted: 2023.05.15
Published: 2023.05.24

Tryptophan-Based Organoclay for Aqueous Naphthol Blue Black Removal – Preparation, Characterization, and Batch Adsorption Studies

Julinawati Julinawati[1], Febriani Febriani[1], Irfan Mustafa[1], Fathurrahmi Fathurrahmi[1], Rahmi Rahmi[1], Sheilatina Sheilatina[1], Khairunnas Ahmad[1,2], Kana Puspita[3], Muhammad Iqhrammullah[1,2*]

[1] Department of Chemistry, Faculty of Mathematics and Natural Sciences, Universitas Syiah Kuala, Banda Aceh, 23111, Indonesia

[2] Innovative Sustainability Lab, PT. Biham Riset dan Edukasi, Banda Aceh, 23243, Indonesia

[3] Department of Chemistry Education, Faculty of Education and Teacher Training, Universitas Syiah Kuala, Banda Aceh, 23111, Indonesia

* Corresponding author's e-mail: m.iqhram@oia.unsyiah.ac.id

ABSTRACT

To prevent the serious threat of textile wastewater, researchers have developed adsorption-based wastewater treatment using cheap, yet effective, adsorbent materials. Of which is natural bentonite, that has the advantages for adsorption due to its porous structure and functional groups but still suffers from its low affinity against anionic and hydrophilic azo dyes. Herein, we aimed of improving the affinity by amino acid tryptophan embedment into the locally isolated natural bentonite collected from Aceh Province, Indonesia. The prepared bentonite samples were characterized using Fourier transform infrared, X-ray diffraction, and scanning electron microscopy. Adsorptive removal was performed on naphthol blue black (NBB) in a batch system with variations of contact time, pH, and adsorbent dosage. The isotherm studies were carried out at optimum conditions (contact time=15 minutes; pH 1; adsorbent dosage=0.2 g) with several models including Langmuir, Freundlich, Sips, and Redlich-Peterson isotherm models. The characterization results revealed that the modification altered its functional group, crystallinity, and micro-surface morphology that add more benefits for adsorption. At optimum conditions, 99.2% NBB has been successfully removed from the aqueous solution. The isotherm studies suggested that the NBB adsorption onto the tryptophane-modified natural bentonite was dependent on Sips isotherm model (R^2=0.999; root-mean-square-errors=1.11×10^{-4} mg/g).

Keywords: amino acids; bentonite; diazo dye; freundlich; sips; montmorillonite; textile wastewater.

INTRODUCTION

Naphthol blue black (NBB) is diazo dye and commonly used in textile industry, in which its pollution threat has attracted many researchers to develop a proper treatment. Electrochemical oxidation (Afanga et al., 2021), photodegradation (Surya et al., 2018), enzymatic degradation (Iqhrammullah et al., 2023; Puspita et al., 2022), and membrane distillation (Baghel et al., 2018) are some examples of methods proposed to treat NBB from textile wastewater effluent. The foregoing methods have several drawbacks including requiring complex equipment and expensive maintenance. Alternatively, adsorption is another wastewater treatment method that is quite popular and considered as simple and cheap. In this light, employing bentonite could be perceived as strategic since the material is relatively cheap, abundant in nature, and can be recovered after used in the treatment. Of many examples, the clay and its composite have utilized for water treatment by researchers across the globe (El-kordy et al., 2022; Iqhrammullah et al., 2020; Jaber et al., 2022; Lahnafi et al., 2022). Since our group is based in Indonesia, our works focused on the utilization

of local natural products including bentonite. Some studies have used natural bentonite from Indonesia to treat different pollutants including heavy metal (Kadja and Ilmi, 2019) and synthetic azo dyes (Abdel Salam et al., 2020; Taher et al., 2019). The superiority of bentonite in adsorption is ascribed to its high porosity and contact surface area and rich functional groups. However, its affinity against negatively or neutrally charged and hydrophobic molecules, including protonated NBB, is low. Therefore, in this present study, we have modified the local bentonite with amino acid tryptophan embedment to give more affinity against the NBB. Tryptophan could add new N- and O-functional groups which contribute to the adsorption capacity, hence its high applicability in modifying dye-adsorbing materials (Ahmad et al., 2022; Sahoo et al., 2019; Toledo et al., 2020). Other than the novelty reason, the employment of tryptophan is based on the fact that this amino acid could be recovered from cheap resources such as tofu wastewater (Fathana et al., 2021). To prepare the organoclay, researchers have utilized the cations (such as Na^+) from the interlayer region to be exchanged with the amino acid cations (Chen et al., 2018; Lahnafi et al., 2023). Previous research suggested that free amino acid could form various Coulombic interactions with organic synthetic dyes, namely electrostatic interaction, hydrogen bond, and π-π stacking (Zhang et al., 2020). There have been several studies employing this strategy of embedding amino acids into bentonite (the adsorbent is then commonly referred as organoclay) to improve its performance for adsorptive removal of pollutants (Abdel Salam et al., 2020; Hajjizadeh et al., 2020; Zhou et al., 2019). The innovativeness of our work is that we utilized local natural bentonite from Aceh Province Indonesia, where its modifications along with its utilization to treat anionic dyes are still underreported.

MATERIALS AND METHODS

Materials

Chemicals used in this study were NaCl, L-tryptophan, naphthol blue black (NBB), HCl, and NaOH were analytical grade and purchased from Merck (Selangor, Malaysia). Ca-bentonite was natural bentonite, collected from Desa Teupin Reusep, North Aceh, Indonesia.

Preparation of Tryptophan-Na-bentonite (Tr-Na-Bentonite)

The oven-dried Ca-Bentonite (105°C) was added to a NaCl-containing glass Beaker with a ratio of 1 g:100 mL and subsequently stirred for 24 h (250 rpm; room temperature) to form Na-bentonite. Thereafter, the precipitate was washed with deionized water repeatedly to remove chloride ions (confirmed using AgNO3 test; 4000 rpm). The sample was decanted at room temperature, oven-dried at 105°, and crushed and sieved with a 100-mesh sieve.

To prepare the tryptophane-Na-bentonite (Tr-Na-bentonite) the previously obtained Na-bentonite was dispersed in a solution containing L-tryptophan (0.2 g/g Na-bentonite) so that the ratio between Na-Bentonite and the solution was 1 g: 100 mL. The mixture was left for 24 hours on a shaker at 250 rpm until the Trp-Na-Bentonite was formed. Thereafter, Trp-Na-Bentonite was separated from the mixture by centrifugation and washed with deionized water. The oven-dried precipitate of Trp-Na-bentonite (105°C) was crushed with a crusher and sieved with a 100-mesh sieve.

Characterization

The prepared Trp-Na-bentonite was characterized using Fourier transform infrared (FT-IR) Prestige 21 (Shimadzu, Kyoto, Japan), scanned from 4000 to 450 cm^{-1} for functional group identification. The X-ray diffraction (XRD) pattern was obtained from an analysis using Shimadzu XRD-700 (Kyoto, Japan), in which the conditions used for the X-ray tube were 40 kV and 30 mA (Cu Kα radiation), scanning the sample from 2Θ=10° to 80° with a speed of 2°/minute. Morphological characteristics of the Trp-Na-bentonite surface were observed on scanning electron microscope (SEM) Jeol. Jsm-6510 LA (Tokyo, Japan) at 15 kV with 10,000x magnification.

Batch adsorption of Naphthol Blue Black (NBB)

The batch adsorption studies were performed using Erlenmeyer (250 mL) containing 25 mL NBB treated with adsorbent Trp-Na-bentonite. The Erlenmeyer was then placed on a rotary shaker at 120 rpm and at room temperature. The adsorbent was separated from the treated solution using centrifugation at 400 rpm for 15 minutes.

The filtrate was measured for remaining NBB concentration using UV-Vis spectrophotometer at maximum wavelength (615 nm). The first batch adsorption parameter optimized was contact time, where the contact time varied from 5 to 25 minutes (initial NBB concentration = 10 mg/L; pH 7; adsorbent dosage = 0.2 g). Next, the optimum pH was determined by varying the level from pH 1 to 9 (initial NBB concentration = 10 mg/L; contact time = 15 minutes; adsorbent dosage = 0.2 g). The effect of adsorbent dosage was investigated with a variation from 0.1 to 0.5 g (initial NBB concentration = 2.5 mg/L; contact time = 15 minutes; pH 1). Variation on initial concentration of NBB was also performed with the range of 2.5–20 mg/L (initial NBB concentration = 2.5 mg/L; contact time = 15 minutes; pH 1; adsorbent dosage = 0.2 g). Data from the initial concentration variation were used to construct isotherm models using OriginPro 2021 (OriginLab Corporation Northampton, MA, USA).

RESULTS AND DISCUSSION

Characteristics of Trp-Na-Bentonite

Bulk appearance and micro-surface morphology

The appearances of bulk samples of Na-bentonite and Na-Trp-Bentonite prepared in this study have been presented in Figure 1a and 1b. Except the change in the color tone, where the Na-Trp-Bentonite appeared to have darker color than that of Na-Bentonite, no other differences were found between the two samples. The color change could be associated with the addition of organic content (in this case tryptophan), followed by preparation processes involving several steps of oven-drying.

A deeper analysis of the micro-structure morphology on both samples shows the particles have irregular structures (Figure 1c,d). Flake-like small particles were found more common in Trp-Na-Bentonite than in Na-Bentonite which could be ascribed to the results of crushing steps during the preparation. The presence of pores is more pronounced in Na-Bentonite as compared with that in Trp-Na-Bentonite. The similar findings were also observed by a previous study using glutamate as the modifying amino acids, where higher numbers of small and flake-like particles observed in the modified sample (Hajjizadeh et al., 2020). This indicates the incorporation of amino acid tryptophan increases the particle size, hence reducing the porosity (Figure 1c,d). The change of particle size has been confirmed using ImageJ software based on the suggestion of a previous study (Rahmi et al., 2022b). The averaged diameter of the particle increased from 5.232 to 6.684 μm. Increases on diameter were observed in organoclays modified with amino acids (Zhou et al., 2019). Despite the decrease in porosity, higher NBB uptake could occur with enriched functional group from the amino acids. Therefore, we have investigated the functional groups of Na-bentonite and Na-Trp-Bentonite based on FT-IR. O-containing functional groups have been suggested to facilitate the adsorbate diffusion into the adsorbent particles via increased hydrophilicity and strong affinity with azo dye (Yang et al., 2021). Another study has witnessed that carbonaceous adsorbents enriched with N-containing functional groups could effectively remove azo dyes (included methyl orange, Congo red, crystal violet, and malachite green) from waters (Nguyen et al., 2022).

Functional group

A broad spectral band between 3700 and 3250 cm^{-1} in the spectra of Na-bentonite and Na-Trp-Bentonite is assigned to the stretching vibration of bonded O-H (Figure 2). A small spectral peak at 2508 cm^{-1}, in the spectra of Trp-Na-bentonite, is assigned to the stretching vibration of O-H in carboxylic acid, which belongs to the tryptophan. The successful tryptophane incorporation is also indicated by the presence of C-N from amino acid based on an exclusive spectral peak at 1419 cm^{-1} in the spectra of Trp-Na-bentonite (Kim et al., 2007). At a finger print region, spectral peaks from the stretching vibrations of Si-O-Si (1026–1024 cm^{-1}), Al-Mg-OH (794–793 cm^{-1}), Si-O-Al (544–539 cm^{-1}), as well as Al(Mg)-O-Si (489–466 cm^{-1}) were observed, indicating the typical IR characteristics of bentonite (Figure 2).

The FT-IR analysis revealed the addition of tryptophane contributes to presence of O- (from the carboxylic group) and N-containing functional groups (from the amine group). These functional groups are essential in adsorbent since they could act as binding sites through Coloumbic interactions or complex formation. In a study using cellulose acetate-based polyurethane film, the adsorption of a cationic Pb^{2+} was found to be dependent on the N- and O-functional groups (Fathana et al., 2021; Iqhrammullah et al., 2021).

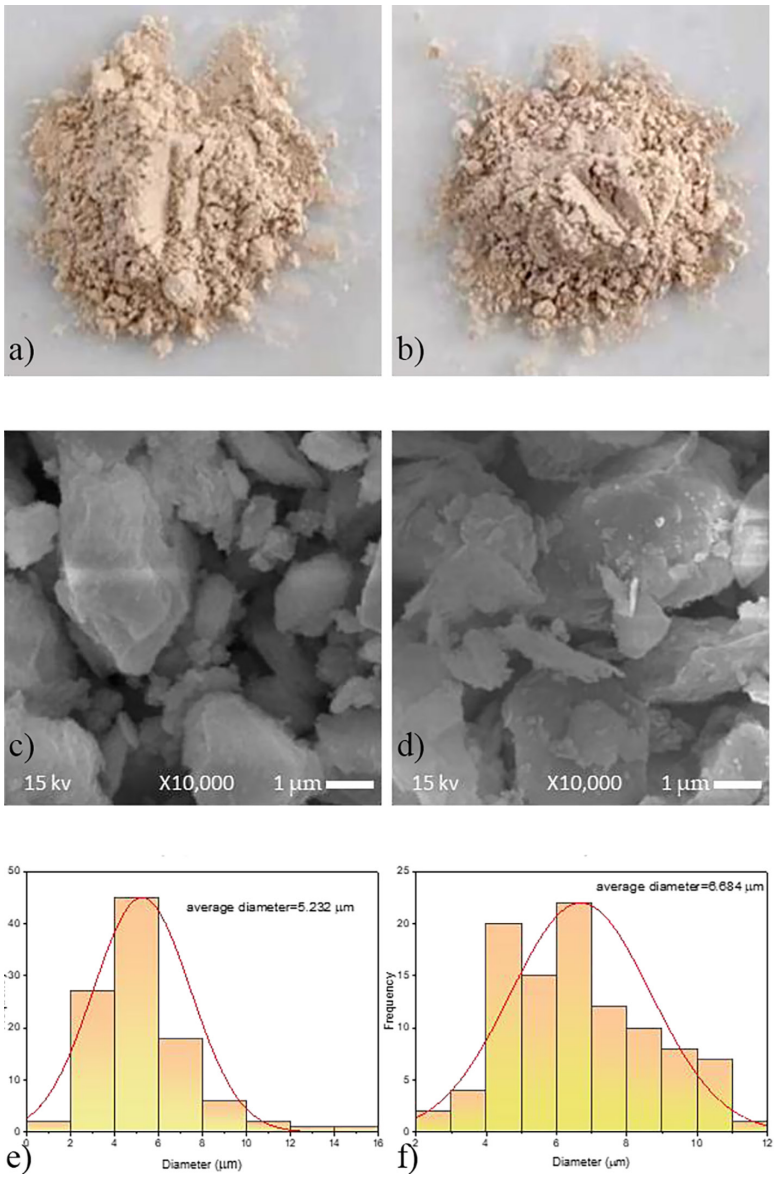

Figure 1. Bulk reducingance of Na-Bentonite (a) and Trp-Na-Bentonite (b). SEM images of Na-Bentonite (c) and Trp-Na-Bentonite (d) observed under 10,000x magnification. Particle size distribution of Na-Bentonite (e) and Trp-Na-Bentonite (f) based on the analysis using ImageJ

Crystallinity

Crystallinity profiles of Na-Bentonite and Trp-Na-Bentonite have been characterized using XRD analysis, where their diffractograms have been presented (Figure 3). A clear crystallinity peak at 2θ = 21° corresponds to a crystalline lattice from montmorillonite (bentonite). Other crystalline peaks observed at 2θ = 36° and 62°, also correspond to the montmorillonite crystalline structure, but the latter only observable in the sample before the tryptophan incorporation. These assignments of crystalline peaks are in accordance with the previous report (Abdel Salam et al., 2020). Silicate minerals, namely quartz and anorthite, were observed based on defined crystalline peaks at 2θ = 26° and 27°, respectively. The presence of those minerals was found in the samples before and after the addition of tryptophan. Other minerals, such as tridymite (2θ = 23°) and halloysite (2θ = 12°), could be observed with weak intensity only in the Na-Bentonite sample. Our findings are similar to reported studies, where bentonite samples generated peaks associated with SiO_2 and Al_2O_3 (Kantesaria and Sharma, 2020).

Decreased intensity of the crystalline peaks obtained in this present study could be ascribed to the decrease in crystallinity of the bentonite

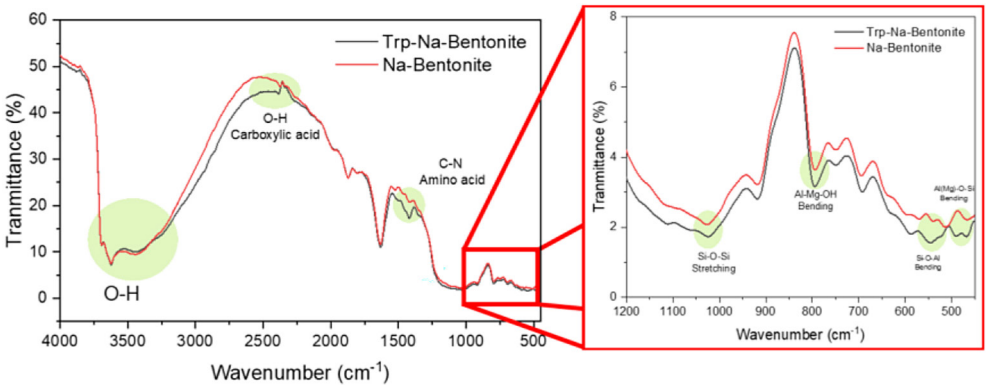

Figure 2. FT-IR spectra of Na-Bentonite and Trp-Na-Bentonite. Left is the zoomed-in presentation of the spectra (1200–450 cm^{-1})

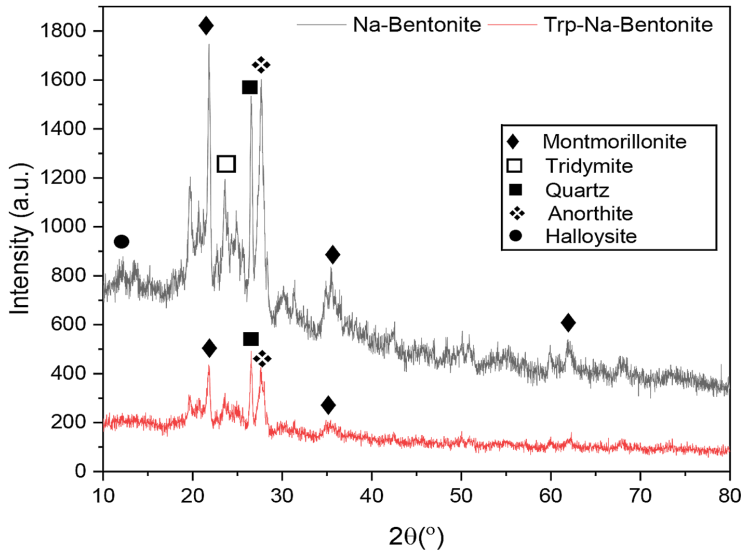

Figure 3. Diffractograms of Na-Bentonite and Trp-Na-Bentonite

sample following the modification with tryptophan. The presence of amino acid tryptophan in may change the interparticle interaction, causing an irregularity in the mineral structure, hence reducing the crystallinity. Such modification of the crystalline structure (higher amorphousness) could be responsible for higher pollutants uptake due to higher water diffusion (Hameed, 2020). The same stipulation was also made by researchers who modified magnetic chitosan for aqueous heavy metal removal (Rahmi et al., 2022b). In addition, the introduction of tryptophan may alter the interlayer spacing in the clay structure as suggested by a study modifying bentonite with glutamic acid (Hajjizadeh et al., 2020). In this present study, the interspace distance in montmorillonite (2θ = 21°) increased from d = 4.07 Å to 4.08 Å, corroborating the successful embedment of tryptophan into the Na-bentonite.

Adsorption of NBB onto Trp-Na-Bentonite

Comparison between Na-Bentonite and Trp-Na-Bentonite in removing NBB

Based on previous characterization, we found that several changes on the Na-Bentonite following the incorporation of tryptophane could be beneficial for NBB removal. Herein, we compared Na-Bentonite and Trp-Na-Bentonite in a batch system for NBB removal. Each adsorbent (0.2 g) was inserted into an Erlenmeyer containing 25 mL NBB 10 mg/L in a pH 7.5 aqueous solution. After 10 minutes of rotary shaking (120 rpm), the removal of NBB reached 9.23% and 17.23% in systems using Na-Bentonite and Trp-Na-Bentonite, respectively (Figure 4). Due to higher adsorption of NBB on Trp-Na-Bentonite than on Na-Bentonite, the former was chosen for the next adsorption studies.

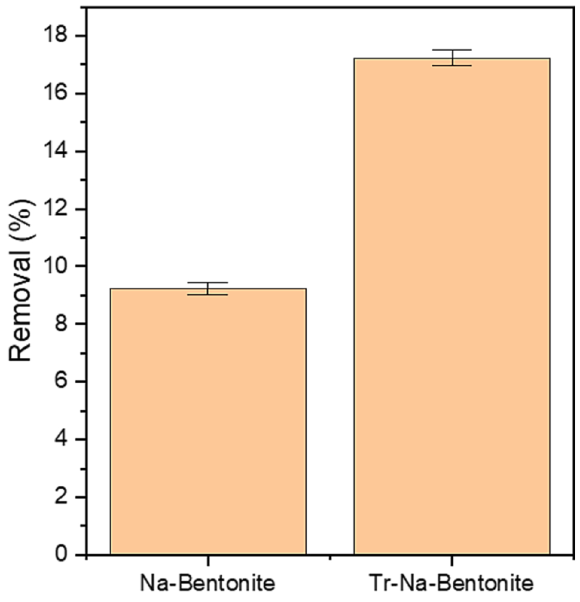

Figure 4. Removal percentages of NBB yielded by Na-Bentonite and Trp-Na-Bentonite in a batch adsorption

Contact time

Effect of contact time on NBB adsorption onto Trp-Na-Bentonite have been presented in Figure 5. The adsorption of NBB could be observed as early as 30 seconds with adsorption capacity reaching 0.0362 mg/g. The adsorption capacity doubled when measured after 1 minute adsorption, and the increase remained significantly until the 3rd minute. Following that, the increase persisted but relatively slow until the equilibrium was reached at the 15th minute. Thereafter, no change was observed with the adsorption capacity. Hence, 15 minutes was taken as the optimum time and used for the next studies.

pH

The effect of initial solution pH on NBB adsorption onto Trp-Na-Bentonite has been presented (Figure 6). When the solution pH was adjusted to pH 1, the adsorption capacity reached 1.15 mg/g. This number sharply depleted when the solution pH was increased to pH 2 and 5 (0.82 and 0.22 mg/g, respectively). These findings are similar to previously published reports, where NBB adsorptive removal was optimum at pH 1 (Ermanda et al., 2021). The adsorption capacity kept on a decreasing trend when the solution pH was more than 5 but relatively small. The effect of pH could be ascribed to the amine group incorporated in the bentonite which could be protonated at low pH. NBB is an anionic dye, hence having negative change and higher affinity with the positively charged adsorbent. The biased result deriving from the possible degradation of NBB was anticipated by comparing the treated sample with reference sample at the same pH level. Therefore, pH 1 was taken as the optimum pH level.

Adsorbent dosage

The effect of adsorbent dosage on the NBB removal by Trp-Na-Bentonite has been presented

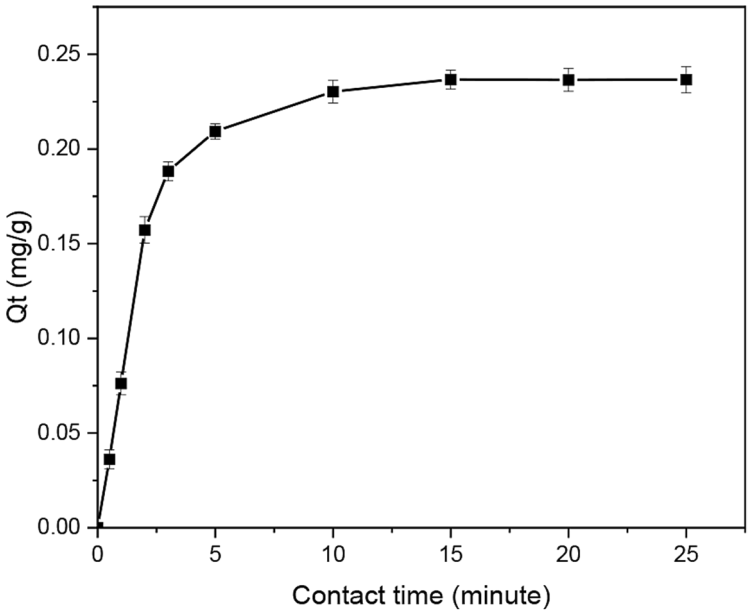

Figure 5. Adsorption capacity of NBB onto Trp-Na-Bentonite observed at various contact time. *Qt* (mg/g) represents adsorption capacity at *t* time

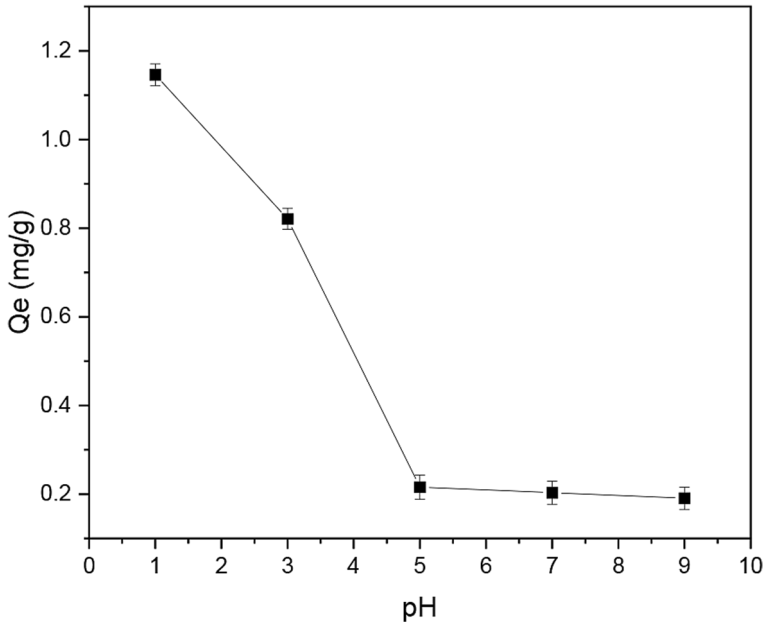

Figure 6. Adsorption capacity of NBB onto Trp-Na-Bentonite observed at various pH levels. *Qe* (mg/g) represents adsorption capacity at the time equilibrium is achieved

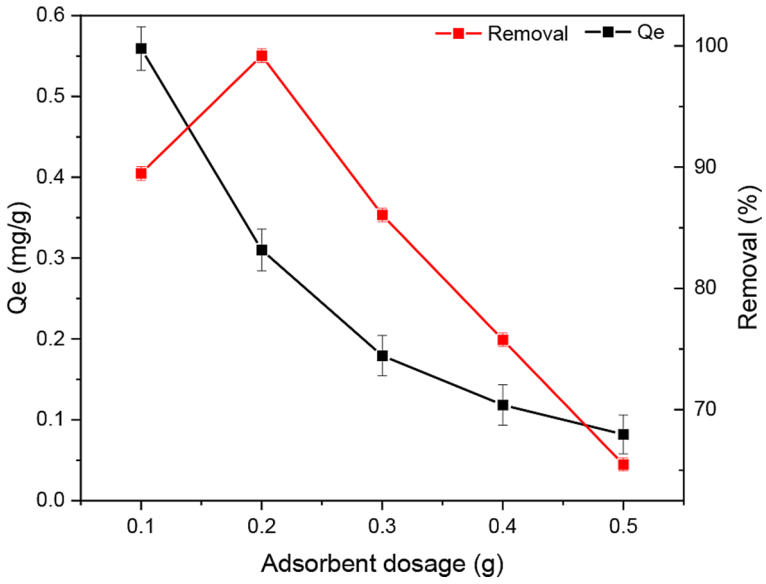

Figure 7. Adsorption capacity and removal percentage of NBB in a batch adsorption system using Trp-Na-Bentonite. *Qe* (mg/g) represents adsorption capacity at the time equilibrium is achieved

in Figure 7. The adsorption capacity appeared in a decreasing trend as the adsorbent dosage was increased. When 0.1 g Trp-Na-Bentonite was used, the adsorption capacity was recorded to be 0.56. By increasing the amount of adsorbent to the system to 0.2, 0.3, 0.4, and 0.5 g, the adsorption capacities were also reduced to 0.31, 0.18, 0.12, and 0.08 mg/g, respectively. Nonetheless, when the dosage increased from 0.1 to 0.2 g, the removal percentage experienced an increase from 89.49% to 99.2%. The different trend of adsorption capacity and removal could be understood by the fact that the adsorption capacity (mg/g) is inversely related to the adsorbent dosage (g). Hence, small adsorbent dosage and high pollutant uptake is the condition for high adsorption capacity. Meanwhile, the removal percentage only depends on the number of pollutant uptake. When the dosage was increased further up to 0.5 g, the removal percentage also experienced a declining trend up to 65.48%. Decreased values on both adsorption capacity and removal percentage in this case is ascribed to the

reduced diffusion force following the first adsorbate concentration decrement. For adsorption efficiency, it is better to take removal percentage as the parameter, hence the 0.2 g as the optimum adsorbent dosage.

Adsorption isotherm

In this study we employed Langmuir and Freundlich models as two-parameters isotherm equations as well as Sips and Redlich-Peterson as three-parameters isotherm models, following the suggestion from a previous study (Tzabar and ter Brake, 2016). Langmuir and Freundlich may predict the nature of adsorbate-adsorbent interactions because the two models used different assumptions. In Langmuir model, the adsorption occurs in monolayer with homogenous energy among the binding sites. Meanwhile, Freundlich model assumes multilayer adsorption with heterogenous binding energy among the binding sites. The fitting curve between the experimental data and theoretical data from each isotherm models is presented in Figure 8.

The fitting parameters and isotherm model parameters have been calculated and are presented in Table 1. The fitness was judged based on R^2 and root-mean-square-errors (RMSE). Note that RMSE also acts as an internal validation factor. According to the two-parameter isotherm model, the data derived from the experiment were in a good agreement with the prediction from Freundlich isotherm model ($R^2 = 0.966$; RMSE = 0.102 mg/g). This means the adsorption favors multilayer adsorption. However, better fitness was obtained when the analysis was carried out using Sips isotherm model ($R^2 = 0.999$; RMSE = 1.11×10^{-4} mg/g). The adsorption capacity-related parameter in this isotherm is K_S, where the value obtained herein is 0.077 (L/g). Since it is a form of combined equation from Langmuir and Freundlich models, the assumption of Sips isotherm might apply differently depending on the adsorbate concentration. The isotherm may favor Freundlich assumptions if the adsorbate concentration range is low (Mozaffari Majd et al., 2022; Tzabar and ter Brake, 2016).

In our previous study, Sips isotherm model was found well-fitted with the Cd^{2+} adsorption onto modified magnetic chitosan which also contained O- and N-functional group (Rahmi et al., 2022a). Anionic methyl orange adsorption on modified chitosan also fitted well with Sips isotherm model (Tanhaei et al., 2020). In a study observing surfactant adsorption on carbonate surface, the data obtained from the experiment were in a good fitness with that predicted by the Sips isotherm model (Kumar and Mandal, 2019). In addition, cationic methylene blue adsorption onto piaçava fibers was suggested to be well predicted by the Sips isotherm model (Marques et al., 2019).

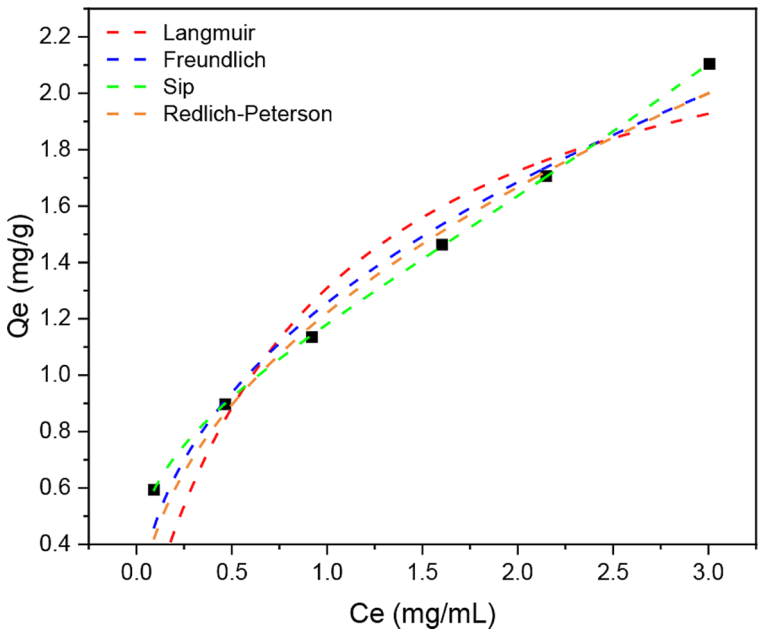

Figure 8. Experimental (■) and theoretical (- - -) data of *Qe* and *Ce* obtained from batch adsorptions of NBB onto Trp-Na-Bentonite with concentration variation (2.5–20 mg/L) at optimum conditions. *Qe* (mg/g) and *Ce* (mg/mL) represent adsorption capacity and final adsorbate concentration at the time equilibrium is achieved, respectively

Table 1. Adsorption isotherm parameters NBB onto Trp-Na-Bentonite

Isotherm models	Parameter	
Langmuir $q_e = \frac{Q_m K_L C_e}{1 + K_L C_e}$	R^2	0.832
	RMSE	0.226 mg/g
	Q_m	2.52 mg/g
	K_L	1.08 L/mg
Freundlich $q_e = K_F C_e^{1/n}$	R^2	0.966
	RMSE	0.102 mg/g
	K_F	1.26 (mg/g) (dm^3/g)^n
	n	2.36
Redlich-Peterson $q_e = \frac{K_R C_e}{1 + a_R C_e^g}$	R^2	0.982
	RMSE	0.055 mg/g
	K_R	1.053 L/g
	a_R	8.63 mg^{-1}
	g	0.55
Sips $Q_e = \frac{K_s C_e^{\beta S}}{1 + as\ C_e^{\beta S}}$	R^2	0.999
	RMSE	1.11×10^{-4} mg/g
	βS	0.026
	$K S$	0.077 (L/g)
	$a S$	0.935 L/mg

Note: β_S – sips isotherm model exponent; a_R – Redlich–Peterson isotherm constant (mg^{-1}); a_S – sips isotherm model constant (L/mg); g – Redlich–Peterson isotherm exponent; K_F – Freundlich isotherm constant related to adsorption capacity (mg/g)(dm^3/g)^n; K_L – Langmuir isotherm constant (L/mg); K_R – Redlich–Peterson isotherm constant (L/g); K_S – Sips isotherm model constant (L/g); Q_m – Langmuir adsorption capacity maximum (mg/g).

STRENGTHS AND LIMITATIONS

This present study is one of a few studies exploring the utility of Indonesia's local clay for wastewater treatment after modified with tryptophan. Moreover, we employed concentration range mimicking that used in industrial setting, particularly textile industry. The adsorbent along with its modifying agent could be obtained from renewable resources. Nonetheless, our study is limited to perform comprehensive characterizations including the specific surface area, volume of the pores, and pores distribution of the Trp-Na-Bentonite and Na-Bentonite. Moreover, the thermal properties of the materials reported in this present study have not been studies. Characterization on the crystalline structure of the material was only based on the XRD analysis, whilst additional structural characterizations such as X-ray fluorescence (XRF) were not performed. Regarding the adsorption performance, our data are not sufficient to establish the kinetic and thermodynamic studies. Herein, we aimed to report the improved adsorptive performance of Indonesian bentonite after modified with tryptophan against an azo dye – NBB. Therefore, we assure the continuation of this study with more strategic modification approach, and more comprehensive studies will be carried out.

CONCLUSIONS

Embedment of NBB into adsorbent Na-Bentonite could improve the NBB removal in a batch adsorption system which could be associated with the addition of O- and N-containing functional group and the increased amorphousness of the adsorbent. The optimum contact time, initial pH level, and adsorbent dosage were 15 minutes, pH 1, and 0.2 g respectively. The NBB adsorption onto Trp-Na-Bentonite is dependent on Sips isotherm model.

REFERENCES

1. Abdel Salam M., Abukhadra M.R., Adlii A. 2020. Insight into the Adsorption and Photocatalytic Behaviors of an Organo-bentonite/Co3O4 Green Nanocomposite for Malachite Green Synthetic Dye

and Cr(VI) Metal Ions: Application and Mechanisms. ACS Omega, 5(6), 2766–2778.

2. Afanga H., Zazou H., Titchou F.E., Gaayda J.E., Sopaj F., Akbour R.A., Hamdani M. 2021. Electrochemical oxidation of Naphthol Blue Black with different supporting electrolytes using a BDD /carbon felt cell. Journal of Environmental Chemical Engineering, 9(1), 104498.
3. Ahmad I., Manzoor K., Aalam G., Amir M., Ali S.W., Ikram S. 2022. Facile Synthesis of L-Tryptophan Functionalized Magnetic Nanophotocatalyst Supported by Copper Nanoparticles for Selective Reduction of Organic Pollutants and Degradation of Azo Dyes. Catalysis Letters, 153, 1–20.
4. Baghel R., Upadhyaya S., Chaurasia S.P., Singh K., Kalla S. 2018. Optimization of process variables by the application of response surface methodology for naphthol blue black dye removal in vacuum membrane distillation. Journal of Cleaner Production, 199, 900–915.
5. Chen H., Chen Q.S., Huang B., Wang S.W., Wang L.Y. 2018. High-potential use of l-Cysh modified bentonite for efficient removal of U(VI) from aqueous solution. Journal of Radioanalytical and Nuclear Chemistry, 316, 71–80.
6. El-kordy A., Elgamouz A., Lemdek E.M., Tijani N., Alharthi S.S., Kawde A.-N., Shehadi I. 2022. Preparation of Sodalite and Faujasite Clay Composite Membranes and Their Utilization in the Decontamination of Dye Effluents. Membranes, 12(5), 12.
7. Ermanda Y., Lubis S., Ramli M. 2021. Preparation and characterization of activated carbon/hematite composite as efficient photocatalyst for naphthol blue black dye degradation, AIP Conference Proceedings, 2342, 060007.
8. Fathana H., Iqhrammullah M., Rahmi R., Adlim M., Lubis S. 2021. Tofu wastewater-derived amino acids identification using LC-MS/MS and their uses in the modification of chitosan/TiO_2 film composite. Chemical Data Collections, 35, 100754.
9. Hajjizadeh M., Ghammamy S., Ganjidoust H., Farsad F. 2020. Amino Acid Modified Bentonite Clay as an Eco-Friendly Adsorbent for Landfill Leachate Treatment. Polish Journal of Environmental Studies, 29(6), 4089–4099.
10. Hameed A.M. 2020. Synthesis of Si/Cu Amorphous Adsorbent for Efficient Removal of Methylene Blue Dye from Aqueous Media. Journal of Inorganic and Organometallic Polymers and Materials, 30, 2881–2889.
11. Iqhrammullah M., Fahrina A., Chiari W., Ahmad K., Fitriani F., Suriaini N., Safitri E., Puspita K. 2023. Laccase Immobilization Using Polymeric Supports for Wastewater Treatment: A Critical Review. Macromolecular Chemistry and Physics, 224, 2200461.
12. Iqhrammullah M., Marlina Hedwig, R., Karnadi I., Kurniawan K.H., Olaiya N.G., Mohamad Haafiz M.K., Abdul Khalil H.P.S., Abdulmadjid S.N. 2020. Filler-Modified Castor Oil-Based Polyurethane Foam for the Removal of Aqueous Heavy Metals Detected Using Laser-Induced Breakdown Spectroscopy (LIBS) Technique. Polymers, 12(4), 903.
13. Iqhrammullah M., Suyanto H., Pardede M., Karnadi I., Kurniawan K.H., Chiari W., Abdulmadjid S.N. 2021. Cellulose acetate-polyurethane film adsorbent with analyte enrichment for in-situ detection and analysis of aqueous Pb using Laser-Induced Breakdown Spectroscopy (LIBS). Environmental Nanotechnology, Monitoring & Management, 16, 100516.
14. Jaber L., Elgamouz A., Kawde A.-N. 2022. An insight to the filtration mechanism of Pb(II) at the surface of a clay ceramic membrane through its preconcentration at the surface of a graphite/clay composite working electrode. Arabian Journal of Chemistry, 15(12), 104303.
15. Kadja T.M.G., Ilmi M.M. 2019. Indonesia natural mineral for heavy metal adsorption: A review. School of Environmental Science, 2(2), 139–164.
16. Kantesaria N., Sharma S. 2020. Exfoliation and Extraction of Nanoclay from Montmorillonite Mineral Rich Bentonite Soil, in: Prashant, A., Sachan, A., Desai, C.S. (Eds.), Advances in Computer Methods and Geomechanics. Springer Singapore, Singapore, 1–12.
17. Kim M., Hwanga S., Yu J.-S. 2007. Novel ordered nanoporous graphitic C3N4 as a support for Pt–Ru anode catalyst in direct methanolfuel cell. Journal of Materials Chemistry, 17, 1656–1659.
18. Kumar A., Mandal A. 2019. Critical investigation of zwitterionic surfactant for enhanced oil recovery from both sandstone and carbonate reservoirs: Adsorption, wettability alteration and imbibition studies. Chemical Engineering Science, 209(14), 115222.
19. Lahnafi A., Elgamou, A., Jaber L., Tijani N., Kawde A.-N. 2023. NaA zeolite-clay composite membrane formulation and its use as cost-effective water softener. Microporous and Mesoporous Materials, 348, 112339.
20. Lahnafi, A. Elgamouz A., Tijani N., Jaber L., Kawde A.-N. 2022. Hydrothermal synthesis and electrochemical characterization of novel zeolite membranes supported on flat porous clay-based microfiltration system and its application of heavy metals removal of synthetic wastewaters. Microporous and Mesoporous Materials, 334, 111778.
21. Marques B.S., Frantz T.S., Sant'Anna Cadaval Junior T.R., de Almeida Pinto L.A., Dotto G.L. 2019. Adsorption of a textile dye onto piaçava fibers: kinetic, equilibrium, thermodynamics, and application in simulated effluents. Environmental Science and Pollution Research, 26, 28584–28592.
22. Mozaffari Majd M., Kordzadeh-Kermani V., Ghalandari V., Askari A., Sillanpää M. 2022. Adsorption isotherm models: A comprehensive and systematic review (2010−2020). Science of The Total Environment, 812, 151334.

23. Nguyen D.T.C., Vo D.V.N., Nguyen T.T., Nguyen T.T.T., Nguyen L.T.T., Tran T.V. 2022. Kinetic, equilibrium, adsorption mechanisms of cationic and anionic dyes on N-doped porous carbons produced from zeolitic-imidazolate framework. International Journal of Environmental Science and Technology, 19, 10723–10736.
24. Puspita K., Chiari W., Abdulmadjid S.N., Idroes R., Iqhrammullah M. 2023. Four Decades of Laccase Research for Wastewater Treatment: Insights from Bibliometric Analysis. International Journal of Environmental Research and Public Health, 20(1), 308.
25. Rahmi, Julinawati, Nina M., Fathana H., Iqhrammullah M. 2022a. Preparation and characterization of new magnetic chitosan-glycine-PEGDE (Fe_3O_4/Ch-G-P) beads for aqueous Cd(II) removal. Journal of Water Process Engineering, 45, 102493.
26. Rahmi R., Lelifajri L., Iqbal M., Fathurrahmi F., Jalaluddin J., Sembiring R., Farida M., Iqhrammullah M. 2022b. Preparation, Characterization and Adsorption Study of PEDGE-Cross-linked Magnetic Chitosan (PEDGE-MCh) Microspheres for Cd^{2+} Removal. Arabian Journal for Science and Engineering, 48, 159–167.
27. Sahoo J.K., Paikra S.K., Mishra M., Sahoo H. 2019. Amine functionalized magnetic iron oxide nanoparticles: synthesis, antibacterial activity and rapid removal of Congo red dye. Journal of Molecular Liquids, 282, 428–440.
28. Surya L., Sheilatina Praja P.V., Sepia N.S. 2018. Preparation and Characterization of Titania/Bentonite Composite Application on the Degradation of Naphthol Blue Black Dye. Research Journal of Chemistry and Environment, 22(2), 48–53.
29. Taher T., Rohendi D., Mohadi R., Lesbani A. 2019. Congo red dye removal from aqueous solution by acid-activated bentonite from sarolangun: kinetic, equilibrium, and thermodynamic studies. Arab Journal of Basic and Applied Sciences, 26, 125–136.
30. Tanhaei B., Ayati A., Iakovlev, E., Sillanpää M. 2020. Efficient carbon interlayed magnetic chitosan adsorbent for anionic dye removal: Synthesis, characterization and adsorption study. International Journal of Biological Macromolecules, 164, 3621–3631.
31. Toledo P.V., Bernardinelli O.D., Sabadini E., Petri D.F. 2020. The states of water in tryptophan grafted hydroxypropyl methylcellulose hydrogels and their effect on the adsorption of methylene blue and rhodamine B. Carbohydrate Polymers, 248, 116765.
32. Tzabar N., Ter Brake H.J.M. 2016. Adsorption isotherms and Sips models of nitrogen, methane, ethane, and propane on commercial activated carbons and polyvinylidene chloride. Adsorption, 22, 901–914.
33. Yang G., Gao H., Lia Q., Ren S. 2021. Preparation and dye adsorption properties of an oxygen-rich porous organic polymer. RSC Advances, 11, 15921–15926.
34. Zhang W., Zhang R.-Z., Yin Y., Yang J.-M. 2020. Superior selective adsorption of anionic organic dyes by MIL-101 analogs: Regulation of adsorption driving forces by free amino groups in pore channels. Journal of Molecular Liquids, 302, 112616.
35. Zhou G., Wang Y., Zhou R., Wang C., Jin Y., Qiu J., Hua C., Cao Y. 2019. Synthesis of amino-functionalized bentonite/$CoFe_2O_4$@MnO_2 magnetic recoverable nanoparticles for aqueous Cd^{2+} removal. Science of The Total Environment, 682, 505–513.